

Reprinted from
6th INT'L. SYMPOSIUM ON RAREFIED GAS DYNAMICS, VOL. 2
©1969, Academic Press, Inc., New York and London

CR

A STUDY OF ROTATIONAL RELAXATION IN A
LOW-DENSITY HYPERSONIC FREE JET BY
MEANS OF IMPACT-PRESSURE MEASUREMENTS[†]

B. Lefkowitz[‡] and E. L. Knuth
Department of Engineering
University of California
Los Angeles, California 90024

ABSTRACT

Rotational-relaxation times obtained for nitrogen using the sudden-freezing criterion are consistent with a model in which (a) the collision number has value unity for temperatures from 10 to 100°K, and (b) rotational transitions occur only if the closest distance of approach is less than 0.993 σ , where σ is the distance at which the intermolecular potential vanishes. In contradistinction to a viscosity cross section, the collision cross section for this model decreases as temperature decreases.

INTRODUCTION

Interest in rotational-translational energy transfers under the conditions encountered in low-density gas expansions has grown rapidly, partly as a consequence of the use of supersonic jets in molecular beams.¹ In an extensive study of nitrogen free jets, Reis² found that, at low densities, the measured impact pressures exceeded predictions. Knuth^{3,4} proposed that these measurements

[†]Based on the Ph.D. Dissertation of the first author (Ref. 38). Supported chiefly by NSF Grant GK-580; also by NASA Grant NsG 237-62.

[‡]Present address: McDonnell Douglas Corp., Santa Monica, California.

page - 19 1421 N71 72501
Code - none
CR - 117445 Sgt-64618

were affected by lags of the rotational degrees of freedom, and described how such measurements could be used to obtain the rotational relaxation time. The electron-beam-fluorescence technique^{5,6} has been used in measurements of rotational temperatures in expanding flows.^{7,8,9,10} Although the relevant excitation-emission processes are not understood fully and quantitative differences exist in the results reported from the different laboratories, this technique can be used to detect rotational lags. Other investigators^{11,12} used the molecular-beam time-of-flight technique coupled with an energy balance and the assumption of adiabatic flow. Campargue¹³ defined a beam-optimization parameter for supersonic molecular beams, showed that it depends on the effective specific-heat ratio, deduced values of this effective specific-heat ratio from beam intensity measurements, and concluded that, for the conditions investigated, the rotational degrees of freedom of hydrogen and deuterium had ceased to participate in the expansion process already at the nozzle throat. Bier and Schmidt¹⁴ noted the effect of rotational lags on the lateral dimensions of the barrel shock formed in a hydrogen free jet.

Relaxations with rotational temperatures, T_r , either nearly equal to or significantly lower than translational temperatures, T_t , have been studied over a longer period of time. Rotational lags have been inferred from ultrasonic absorption and dispersion,^{15,16,17} from changes in the stagnation pressure in the compression of gas from a subsonic jet at the tip of an impact tube,¹⁸ and from changes in the density ratio across a shock wave.¹⁹

Although significant quantitative differences are found in the predictions of the several available analyses of rotational-translational energy transfers, some consistent trends are found also. For single transitions, both Brout²⁰ and Raff²¹ predict that the collision number, N_r , decreases as the translational temperature increases. For multiple transitions, both Widom²² and Sather and Dahler²³ predict that N_r is independent of temperature

for rigid molecules with no attractive potentials whereas both Parker²⁴ and Sather and Dahler²⁵ predict that N_r increases as temperature increases for molecules with attractive-repulsive potentials. Note that, contrary to some other analyses, each of the latter four analyses²²⁻²⁵ uses a single molecular model for predicting both the relaxation rate and the collision rate.

The present data are interpreted by assuming that the rotational degrees of freedom froze at the axial location at which the measured impact pressure begins to deviate from the impact pressure predicted^{26, 27} for isentropic free-jet expansions and measured^{28, 29, 30} under conditions for which local translational-rotational equilibrium is expected. The rotational-relaxation time τ_r is calculated using a sudden-freezing criterion similar to the criteria used, e. g., for atom recombinations³¹ and for vibrational relaxations.³²

APPARATUS

The apparatus, consisting essentially of a system for producing a free jet, a mechanism for positioning the jet, and an impact tube for measuring impact pressures, is depicted schematically in Figure 1. The position of the stagnation chamber was set by a rotary feed-through attached to a micrometer head and indicated by a dial attached to the feed-through. Stagnation-chamber temperature was equated to the room temperature measured by a mercury thermometer. Stagnation-chamber pressure was measured by a diaphragm-type strain-gage pressure transducer. Jet ambient pressures from about 5.5×10^{-5} to 4.3×10^{-4} torr were realized.

In order to avoid probe-displacement effects, low-density effects, and long response times, an impact tube with $\frac{1}{2}$ -in. length, 0.018-in. OD, 0.010-in. ID, and 10° external chamfer was used. A response time of 25 sec was estimated.³³ Low-density effects were avoided by avoiding impact-tube Knudsen numbers greater than unity. Impact-tube pressures were measured with a diaphragm-

type capacitive pressure transducer.

PROCEDURE

Impact pressures were measured at several nozzle-probe distances for both nitrogen and argon. Mach-disk effects were avoided by keeping the nozzle-probe distance small in comparison with the distance from the nozzle to the Mach disk as measured by Bier and Schmidt.¹⁴ Measurements at a given stagnation pressure were used only if the zero-point outputs of the probe and stagnation-chamber transducers drifted respectively less than 3×10^{-3} and 2×10^{-2} torr during the measurements.

Measured impact pressures were compared with impact pressures predicted for isentropic free-jet expansions using centerline Mach-number calculations²⁷ and impact pressure vs. Mach number calculations.³⁴ Measured impact pressures were corrected as indicated in the following paragraphs.

Measured shock-detachment distances are available^{35, 36} for a diatomic gas flowing over a flat-nosed body of revolution at several different Mach numbers. Since the values predicted³⁶ for a heat-capacity ratio of 7/5 agreed well with these measured values (cf. Figure 3), the values predicted³⁶ for heat-capacity ratios of 5/3 and 7/5 (cf. Figure 2) were used here.

The effective orifice diameter, D^* was determined by comparing (a) the measured flow rate with the flow rate predicted for a nonviscous fluid, and (b) the measured impact pressure with the impact pressure predicted for a nonviscous fluid. Results, and the faired curve used in the data analysis, are presented in Figure 3.

The effective source location, x , was determined by comparing the measured impact pressure with the impact pressure predicted for a nonviscous fluid which flows through the orifice with parallel streamlines. Results, and the faired curve used in the data analysis, are presented in Figure 4.

SIXTH RAREFIED GAS DYNAMICS

Viscous effects at the probe were determined by comparing the measured impact pressure, P_I^e , with the impact pressure, P_I^i , predicted for a nonviscous fluid. Ratios of measured and predicted impact pressures were compared for two different stagnation pressures, p_0 , but the same probe Reynolds number. If the two ratios differed, then the largest ratio (affected perhaps by rotational lags) was omitted. The resulting correction curve is given in Figure 5.

In order to verify that the measurements of Figure 5 are free from rotational-lag effects, typical nitrogen measurements believed to be free of rotational-lag effects were compared with argon measurements. The pressure coefficient C_μ (cf. Figure 6) was used³⁷ in order to handle the difference in heat capacities. The correlation of Figure 6 supports the conclusion that Figure 5 is free from rotational-lag effects.

RESULTS

Preliminary nitrogen and argon measurements were motivated by reports that, at the same p_0 and orifice-probe distance, no difference in impact pressures could be detected. At probe Reynolds numbers greater than 25, impact pressures were found to be about 10 percent greater for argon. Hence, confidence in impact-tube studies of rotational freezing was strengthened.

Centerline impact pressures were surveyed then for several values of p_0 . Results for $p_0 = 2.5$ torr are shown in Figure 7. (Results for $p_0 = 2.5, 5, 10, 15, 20, 25, 45,$ and 65 torr are reported graphically by Lefkowitz³⁸ and available in tabular form from the Molecular-Beam Laboratory, UCLA.) The point at which the data begin to deviate from Figure 5 is called the freezing point.

Increases in impact pressures due to freezing of rotational degrees of freedom are significantly greater than the deviations from Figure 5 indicated, e.g., in Figure 7. Although Knuth³ has predicted that rotational freezing can increase the probe Reynolds number by as much as 49

percent, these effects were neglected in the abscissa of Figure 7.

The several values of the dimensionless freezing-point distance $(x^1/D^*)_f$ determined from the impact-pressure data are plotted as a function of the dimensionless freezing-point parameter $D^*/\tau_{ro}a_o$ in Figure 8. Here x^1 is the distance from the effective source to the shock wave, a is the speed of sound, and the subscript o refers to stagnation conditions. Values of $D^*/\tau_{ro}a_o$ were calculated using

$$\frac{D^*}{\tau_{ro}a_o} = \frac{1}{N_{ro}} \left(\frac{8}{\pi\gamma} \right)^{\frac{1}{2}} \frac{\sqrt{2} p_o \pi r_m^2 \Omega_{\mu} D^*}{k T_o} \quad (1)$$

where γ is the specific-heat ratio, p is pressure, k is Boltzmann's constant, T is temperature, r_m is the distance between molecules at minimum intermolecular potential energy, and Ω_{μ} is a factor which handles deviations of viscosity cross sections from rigid-sphere cross sections. $N_r = 5.3$, given by Greenspan,³⁹ and values of r_m and Ω_{μ} tabulated by Hirschfelder, Curtiss, and Bird⁴⁰ were used. Several freezing points determined from the spectroscopic data of Marrone,⁷ using the freezing criterion $dT_r/dx = 0.5 dT/dx$ suggested by Phinney,⁴⁰ are plotted in the same figure.

In order to facilitate the determination of the temperature dependence of τ_r , the sudden-freezing criterion $DT/Dt = -T/\tau_r$ was written, for isentropic flow of a perfect gas, in the form

$$(\gamma-1)M^2 \left(1 + \frac{\gamma-1}{2} M^2 \right)^{\frac{\gamma-2}{\gamma-1}} \frac{dM}{d(x/D^*)} = \frac{D^*}{\tau_{ro}a_o} \frac{N_{ro}}{N_r} \frac{\Omega_r}{\Omega_{ro}} \quad (2)$$

where Ω_r is a generalization of the Ω_{μ} appearing in Equation (1) in that it is not necessarily the viscosity-cross-section factor. For a given gas, the left-hand side of

Equation (2) is a function of x/D^* only. The value of the temperature-dependent ratio $N_r \Omega_{r0} / N_{r0} \Omega_r$ is obtained by dividing, for a measured value of $(x'/D^*)_f$, the measured value of $D^*/\tau_{r0} a_0$ by the calculated value of the left-hand side of Equation (2). A value can be ascribed to either N_r or Ω_r only if the value of the other parameter is adopted a priori.

Values of the cross-section ratio Ω_{r0}/Ω_r obtained using the methods of the preceding paragraph and assuming that $N_r/N_{r0} = 0.16$ in the investigated temperature range (below 100°K) are given in Figure 9. The data are compared with the straight line $\Omega_{r0}/\Omega_r = \exp 0.0575 (T_0/T - 1)$.

DISCUSSION OF RESULTS

Although τ_r is related more closely to the experimental observations, N_r is more convenient in considerations of molecular models. Rowlinson⁴¹ suggests that the Ω_r required to separate N_r from τ_r be based on a criterion of closeness of approach. If he counts only those collisions in which the closest distance of approach is less than r , and if r is less than σ , then he obtains

$$\frac{\Omega_{r0}}{\Omega_r} = \exp \frac{V(r)}{kT_0} \left(\frac{T_0}{T} - 1 \right) \quad r < \sigma \quad (3)$$

where $V(r)$ is the intermolecular potential at the intermolecular distance r . A comparison of Equation (3) with the straight line of Figure 9 indicates that for the investigated temperatures (below 100°K), if $N_r/N_{r0} = 0.16$, then $V(r)/kT_0 = 0.0575$. Using a Lennard-Jones 6-12 intermolecular potential with $\sigma = 3.68 \text{ \AA}$ and $\epsilon/k = 91.5^\circ\text{K}$, where $-\epsilon$ is the minimum value of $V(r)$, one finds that this value of $V(r)$ occurs at $r = 0.993 \sigma$. In other words, for the range of conditions investigated here, rotational transitions occur only if the closest distance of approach is less than 0.993σ .

According to the forementioned Rowlinson model, if $r < \sigma$, then Ω_r decreases as T decreases since low-velocity molecules fail to make effective collisions. The effect of this T dependence can be large at low T . For example, $\Omega_r(T_0)/\Omega_r(10^\circ\text{K}) = 5.3$.

The assumption that $N_r/N_{r0} = 0.16$ (i.e., that N_r is of order unity) is consistent with the data obtained by Miller and Andres.⁴² Using a hard-sphere molecular model, one finds from their data that N_r decreases to the order of unity as T decreases to about 80°K (the lowest T which they investigated). (In principle, the Rowlinson model is equivalent to the hard-sphere model for the special case in which one counts only those collisions with closest distance of approach less than σ . In practice, the Rowlinson model used here differs negligibly from the hard-sphere model if $T \gg 20^\circ\text{K}$.) Since unity is physically a lower limit for N_r , this value is used here down to 10°K . The fact that this value is less than $15/8$, the translational relaxation number obtained⁴² for translational relaxation in a free jet, is of no concern since different collision models are used in these two analyses.

Use of the Rowlinson model obviates the need to use the viscosity cross section — and hence the need to ascribe properties to the viscosity cross section which contradict properties derived by other means. Hamel and Willis⁴³ found, e.g., that if a viscosity cross section is used, then (contrary to other evidence) its value must decrease with T in order to bring their predictions into agreement with the relatively low temperature data of Marrone.⁷

Values of N_r obtained from free-jet expansions (with $T_r > T_t$) appear to be smaller than obtained from ultrasonic dispersions or shock compressions (with $T_r \lesssim T_t$). Similar results have been observed^{44, 45, 46} for vibrational relaxation numbers. These differences merit further studies.

SIXTH RAREFIED GAS DYNAMICS

REFERENCES

1. A. Kantrowitz and J. Grey, Rev. Sci. Inst. 22:328-332, May 1951.
2. R. H. Reis, Princeton U., Report No. FLD-7, May 1962.
3. E. L. Knuth, U. of California (Los Angeles) Report No. 64-53, November 1964.
4. E. L. Knuth, Applied Mechanics Reviews 17:751-762, October 1964.
5. E. P. Muntz, U. of Toronto, UTIAS Report No. 71, April 1961.
6. E. P. Muntz, S. J. Abel, and B. L. Maguire, IEEE Conference on Aerospace, Houston, Texas, July 1965.
7. P. V. Marrone, Physics of Fluids, 10:521-538, March 1967.
8. F. Robben and L. Talbot, Physics of Fluids 9:644-662, April 1966.
9. M. Yasuhara, U. of Southern California, USCAE Report No. 103, August 1966.
10. R. S. Hickman, U. of Southern California, USCAE Report No. 104, September 1966.
11. O. Hagen and W. Henkes, Z. für Naturforschung 15a:851-858, October 1960.
12. D. R. Miller and R. P. Andres, J. Chem. Phys. 46:3418-3423, 1 May 1967.
13. R. Campargue, in Molecular Relaxation Processes (M. Davies, ed.), New York, Academic Press, 1966.
14. K. Bier and B. Schmidt, Z. für angewandte Physik 13:493-500, November 1961.
15. K. F. Herzfeld and T. A. Litovitz, Absorption and Dispersion of Ultrasonic Waves, New York, Academic Press, 1959.
16. T. L. Cottrell and J. C. McCoubrey, Molecular Energy Transfer in Gases, London, Butterworths, 1961.
17. W. P. Mason, Physical Acoustics, Principles and Methods, New York, Academic Press, 1965.

REFERENCES (Continued)

18. H. H. Huber and A. Kantrowitz, J. Chem. Phys. 15:275-284, May 1947.
19. K. Hansen, D. F. Hornig, B. Levitt, M. Linzer, and B. F. Myers, Rarefied Gas Dynamics (L. Talbot, ed.) 593-602, New York, Academic Press, 1961.
20. R. Brout, J. Chem. Phys. 22:1189-1190, July 1954.
21. L. M. Raff, J. Chem. Phys. 46:520-531, 15 January 1967.
22. B. Widom, J. Chem. Phys. 32:913-923, March 1960.
23. N. F. Sather and J. S. Dahler, J. Chem. Phys. 35:2029-2037, December 1961.
24. J. G. Parker, Physics of Fluids 2:449-462, July-August 1959.
25. N. F. Sather and J. S. Dahler, J. Chem. Phys. 37:1947-1951, 1 November 1962.
26. P. L. Owen and C. K. Thornhill, Aeronautical Research Council, R and M 2616, September 1948.
27. F. S. Sherman, personal communication. Results are summarized in Lockheed Missiles and Space Co., Technical Report: Fluid Mechanics 6-90-63-61, 23 May 1963.
28. H. Ashkenas and F. S. Sherman, Rarefied Gas Dynamics (J. H. de Leeuw, ed.) II:84-105, New York, Academic Press, 1966.
29. V. H. Reis and J. B. Fenn, J. Chem. Phys. 39:3240-3250, December 1963.
30. J. B. Fenn and J. Deckers, in Rarefied Gas Dynamics (J. A. Laurmann, ed.) I:497-515, New York, Academic Press, 1963.
31. K.N.C. Bray, J. Fluid Mech. 6:1-32, July 1959.
32. R. Phinney, AIAA J. 1:496-497, February 1963.
33. S. A. Schaaf and R. R. Cyr, J. Appl. Phys. 20:860-863, September 1949.
34. C. J. Wang, J. B. Peterson, and A. Anderson, Space Technology Laboratories, Inc., GM-TR-154, March 1957.

SIXTH RAREFIED GAS DYNAMICS

REFERENCES (Continued)

35. H. W. Liepmann and A. Roshko, Elements of Gas Dynamics, New York, Wiley, 1960.
36. H. Serbin, The Aeronautical Quarterly 9:313-330, November 1958.
37. F. Homann, NACA TN-1344, June 1952.
38. B. Lefkowitz, U. of California (Los Angeles), Report No. 67-27, July 1967.
39. M. Greenspan, J. Acoust. Soc. Amer. 31:155-160, February 1959.
40. R. Phinney, Martin Marietta Co. (Baltimore), RM-172, April 1964.
41. J. S. Rowlinson, Molecular Physics 4:317-320, April 1961.
42. E. L. Knuth and S. S. Fisher, J. Chem. Phys. 48:1674-1684, 15 February 1968.
43. D. R. Willis and B. B. Hamel, in Rarefied Gas Dynamics (C. L. Brundin, ed.) I:837-860, New York, Academic Press, 1967.
44. I. R. Hurle, A. L. Russo, and J. G. Hall, J. Chem. Phys. 40:2076-2089, April 1964.
45. R. F. Duffy, Proceedings of the First International Congress on Instrumentation in Aerospace Facilities, Paris, France, September 1964.
46. D. I. Sebacher, in Proceedings of the 1966 Heat Transfer and Fluid Mechanics Institute (M. A. Saad and J. A. Miller, eds.) 315-334, Stanford, Stanford University Press, 1966.

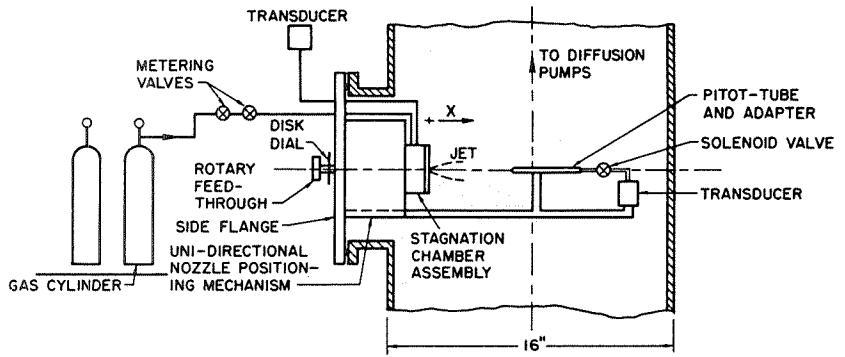


Fig. 1 Schematic diagram of experimental apparatus

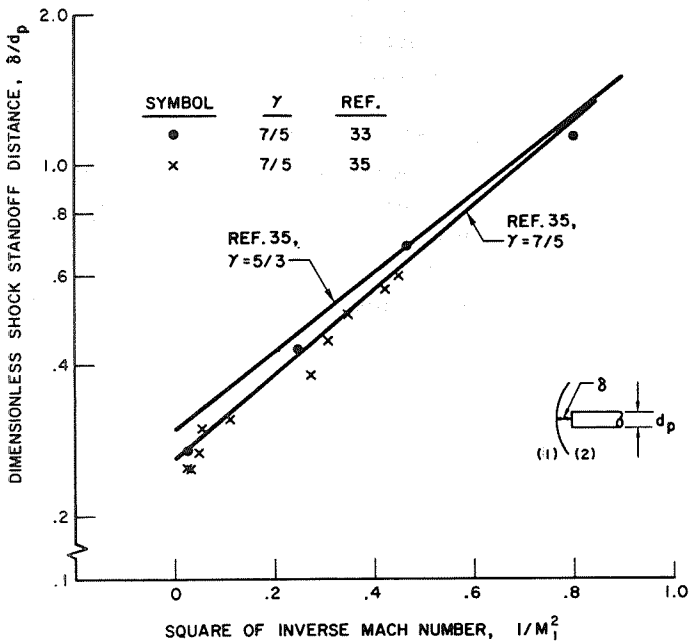


Fig. 2 Correction for shock detachment at probe

SIXTH RAREFIED GAS DYNAMICS

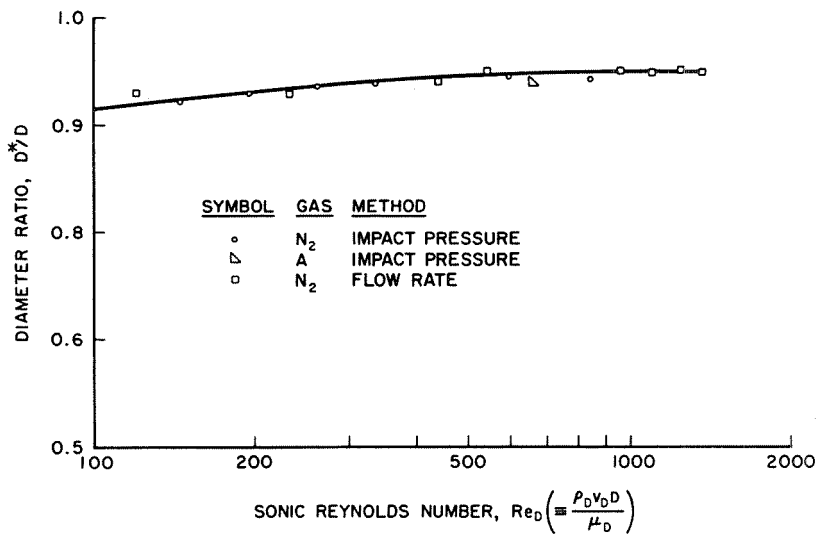


Fig. 3 Correction for diameter of effective orifice

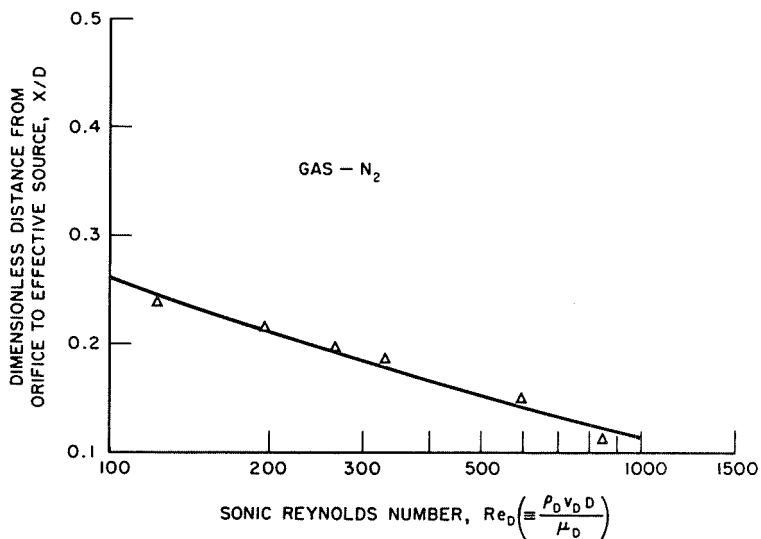


Fig. 4 Correction for location of effective source

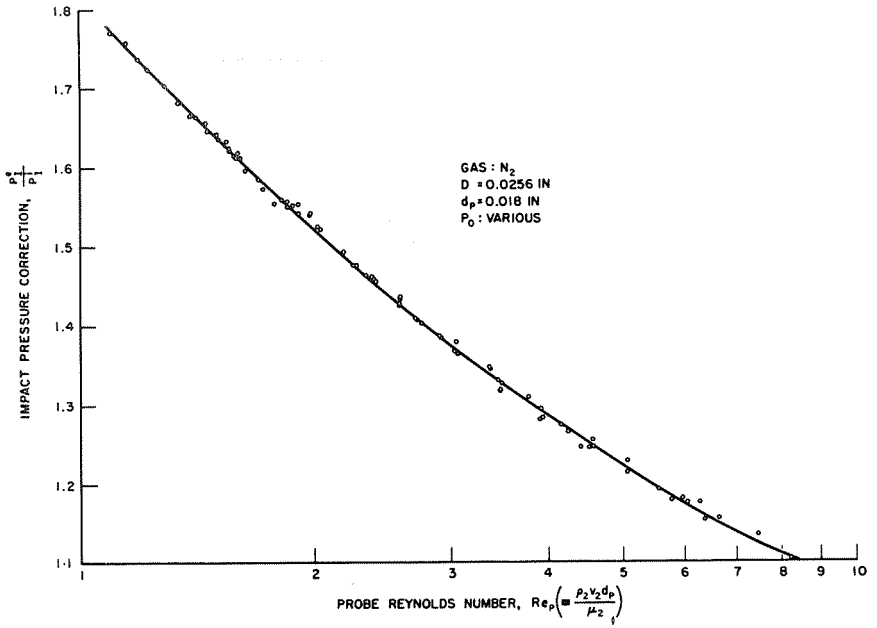


Fig. 5 Impact-pressure correction data (effects of rotational relaxation absent)

SIXTH RAREFIED GAS DYNAMICS

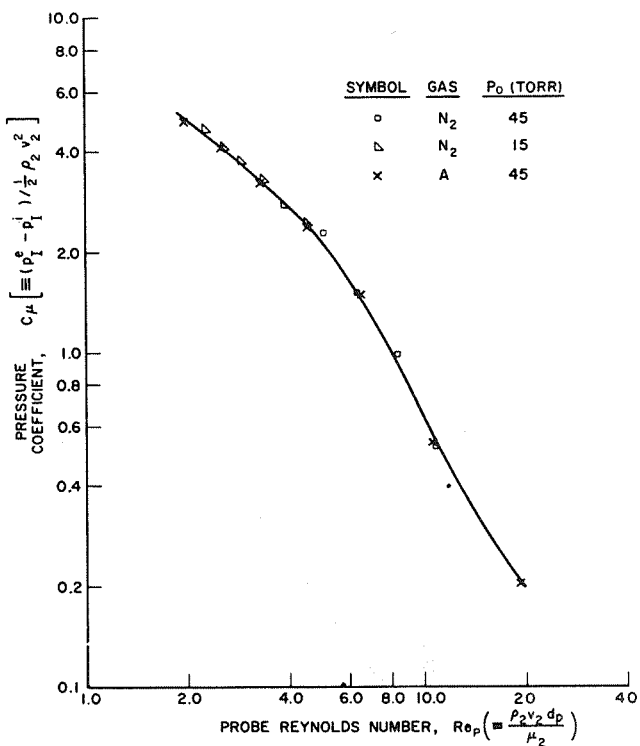


Fig. 6 Pressure coefficient C_μ versus probe Reynolds number (effects of rotational relaxation absent)

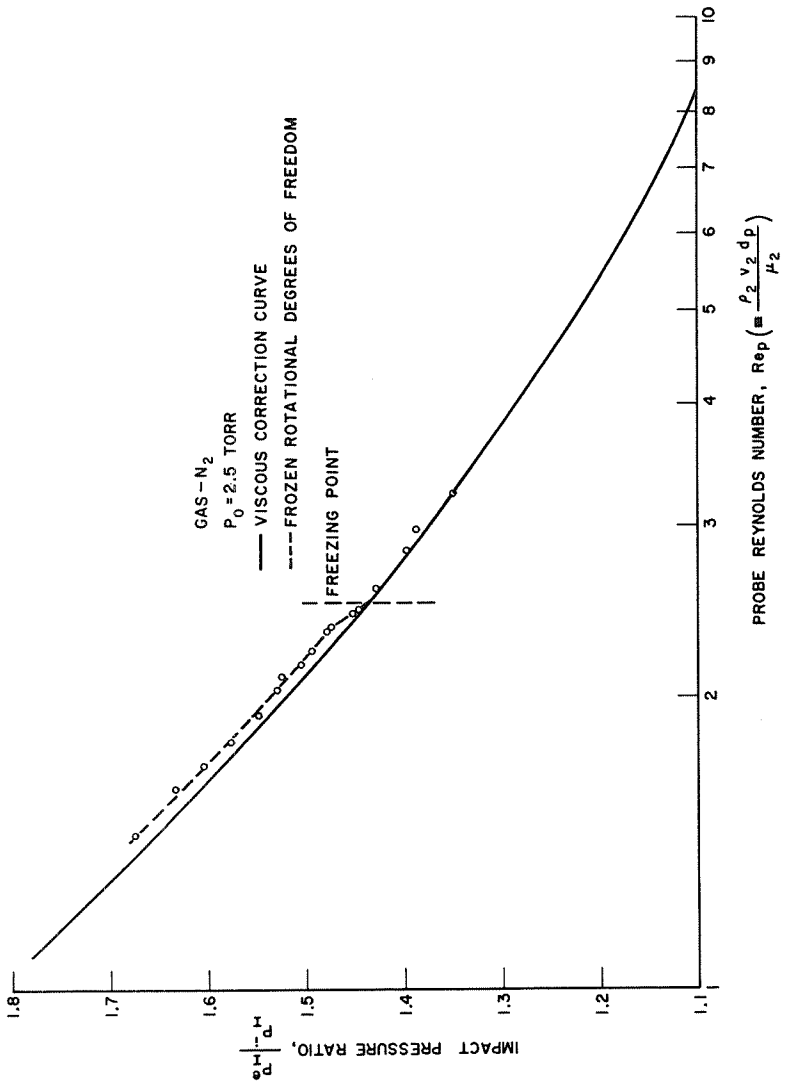


Fig. 7 Impact-pressure ratio versus probe Reynolds number

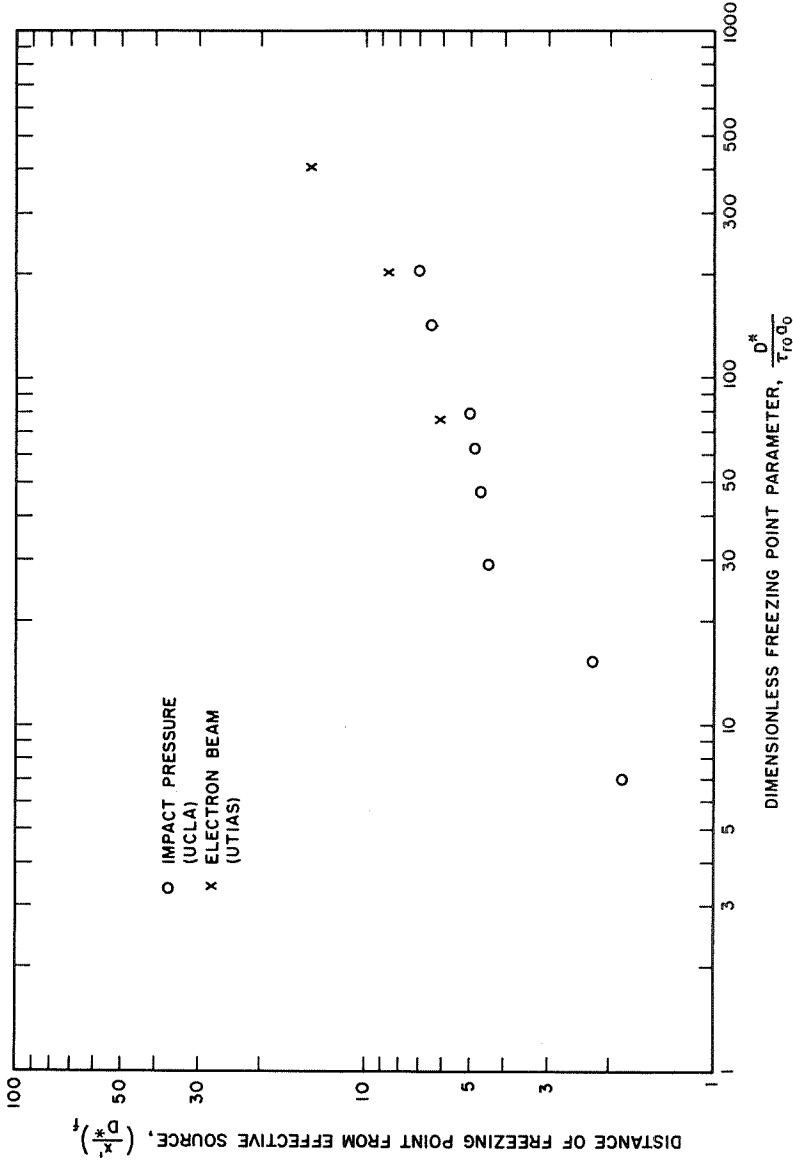


Fig. 8 Freezing-point distance $(x'/D^*)_f$ versus dimensionless freezing-point parameter $(D^*/\tau_{fo}a_0)$

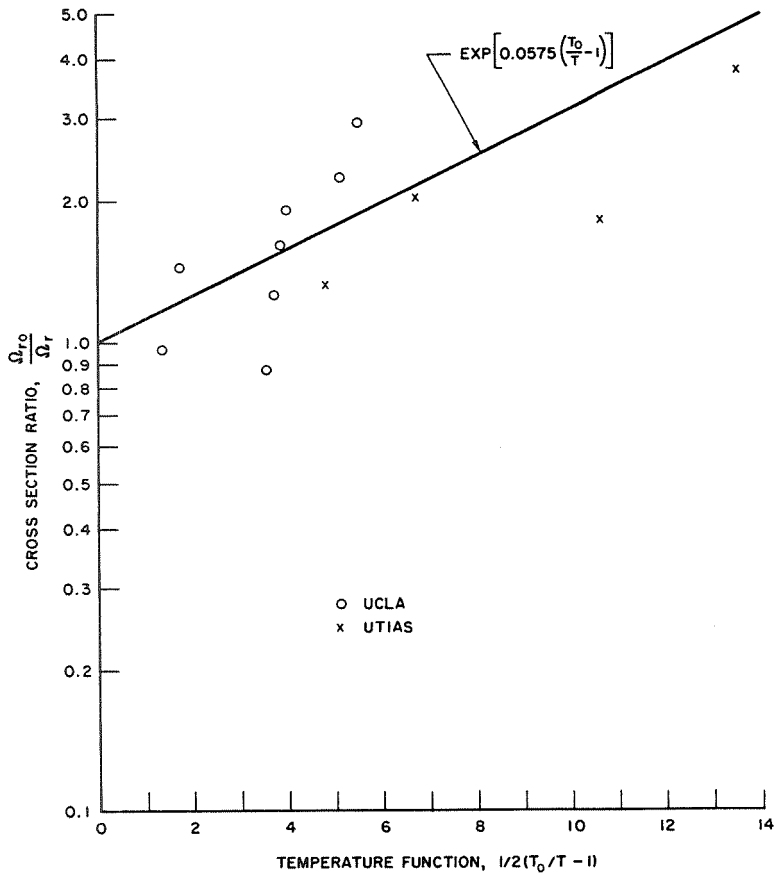


Fig. 9 Temperature dependence of the rotational relaxation cross section